euronoise

Theoretical justification of a coherent forward model for subbottom profiler data inversion

Sandrine Rakotonarivo[a], Michel Legris[a], Rozenn Desmare[b] and Frédéric Jean[c]

[a]Laboratoire E3I2, ENSIETA, 2, rue François Verny, 29806 Brest, France
[b]Institut de Recherche de l'Ecole Navale, IRENav, BP 600, 29240 Brest Armées, France
[c]IXSEA, 46, quai François Mitterrand, 13600 La Ciotat, France
rakotosa@ensieta.fr

Subbottom profiling systems measure and identify sediment layers that exist below the sediment/water interface. Nowadays, very-high resolution chirp profilers provide calibrated wideband signals which may enable quantitative seabed characterisation. In literature, sediment classification is based on attenuation and reflectivity estimation and backscattering models used for the inversion consider plane wave propagation through layered homogeneous attenuated bottom. But this bottom modelling may be in contradiction with the emitted spherical front wave and core samples observations which point out a heterogeneous structure of marine subbottom. Therefore, impacts of profiler features, geometry measurement and subbottom structure (layering, attenuation, rugosity, and volumetric inhomogeneity) on backscattering signal are all reviewed in this paper. This analysis shows that classical model of wave coherent propagation through layered homogeneous attenuated media offers the best compromise between its accuracy and inversion possibility, if bottom heterogeneities are insignificant (Rayleigh scatterers). For bigger heterogeneities (Rayleigh parameter close to unity), coherent backscattering still prevails though wave propagation is affected by scattering. In this case, the same coherent forward model is used with modified reflectivity and transmission coefficients. Then, sensibility and inversion possibility of the coherent bottom backscattering model are discussed.

1 Introduction

Quantitative seabed characterization using very high-resolution profilers is based on the inversion of a backscattering model. Three sediment parameters might be determined from this operation: attenuation, reflection loss and thickness (in term of two way travel times) of detected layer. Then, physical seabed attributes (porosity, susceptibility, celerity, permeability, density, etc…) can be deduced from these three parameters using Hamilton correlation relationships [1]. Accuracy of estimation depends thereby on the rightness of the backscattered model and its inversion ability. Forward wave propagation models into sediment suppose that the subbottom can be described as a layered homogeneous attenuated media with plane and perfect smooth interfaces [2]. These hypotheses may be in contradiction with sediment cores samples observations which show a heterogeneous structure of marine subbottom. Therefore, this paper analyse the acoustic return field with subbottom profiling system in order to justify modelling of wave backscattering by marine sediment bottom. First part of this paper reviews chirp sonar features and marine sediment structure in order to justify hypothesis of the backscattering model and to determine prevailing parameters. Then, impact of each parameter on wave propagation is studied and coherent forward model is presented. Sensibility and inversion possibility of the coherent backscattering model are finally discussed in the last section.

2 Study positioning and hypothesis

2.1 Subbottom chirp profiler

Present subbottom profilers use linear FM pulse for frequencies typically covering the bandwidth [1-10] kHz. This low frequency bandwidth ensures signal to penetrate into soft bottom and to identify them. As subbottom profiling systems work at normal incidence in monostatic configuration, the specular backscattering prevails and the backscattering strength typically computed from forward signal coincides with the reflection coefficient at normal incidence. Moreover, only buried sediment layers perpendicular to the emitted beam may be detected by chirp profilers [3], as they are sensitive to specular return. In consequence, if a lower stratum is visible on profiling, then higher layers are also parallel to this lower stratum and perpendicular to the acoustic beam. At normal incidence, the seafloor can be suitably approximated as a fluid medium as the longitudinal wave is the most favoured in this direction and the transversal wave negligible. As the aperture of chirp sonar is generally wide, the emitted field can be assimilated as a spherical wave's field with geometrical attenuation. For smooth and slightly rough interfaces, sources image theorem can be used to calculate forward field [4]. In the case of very heterogeneous media, any workable signal can be measured by chirp bottom profiler as scattering effects predominate. Influence of fairly rough interfaces on return signal is examined in paragraph 3.3.

2.2 Marine sediment subbottom

In this section, the link between the geologic structure of subbottom from continental shelf and its acoustic description is done in order to get a better understanding of acoustic parameters influencing the backscattered response with chirp system. As chirp profiling system penetrates the only first hundred meters, examined sediments are unconsolidated; and most of them are made of sand, silt and clay which are absorbant.

From sediment depositional analyses and stratigraphy studies [5], some generic remarks concerning vertical arrangement of sediment have been deduced:

- Surficial and burial structure of seafloor is strongly layered and layering scale vary from millimeter (layer) to meter (bed).
- Conformable sediment enchainment respects Steno's law which point out an originally horizontal stratification and an initial lateral continuity strata.

Thus, subbottom profiler is able to distinct an acoustic bed regarding with lithologic parameters wich may correspond to a particular facies. Then interne structure of an acoustic bed may be composed of microlayers and can be viewed as homogeneous if physical properties do not change enough between layer and inhomogeneous if physical properties change continuously. Granular structure of sediment may not influence the acoustic field as $a \leq 2mm < a_0$ (a mean grain size): $ka_0 = 1$ if $a_0 = 239$ mm at 1 khz and $a_0 = 24$ mm at 10 khz. Interfaces between two facies may be rough depending on erosion or grain size during sediment depositional.

Profiler sensitivity to specular reflection and layered structure of subbottom explain use of multilayered backscattering model which is the only model both potentially invertible and representative of seafloor behaviour. Moreover, classical models take into account stratification and attenuation, whereas rough surfaces and inhomogeneous beds may impact on wave propagation. Those all sediment parameters are treated in the next section.

3 Bottom acoustic parameters

3.1 Layering

As stated in section 2.1, chirp profiler configuration enables to use source-image theorem for assessing coherent backscattering by smooth or slightly rough surfaces. For a single interface, geometrical attenuation is inserted in the expression of return signal via term 1/r, r being distance to the source. With stratification, bounds of acoustic beam change when transmitted to the underlying bed (Fig. 1); hence spherical front wave becomes ellipsoidal and expression of geometrical attenuation is not anymore 1/r but $1/(r\,\Delta\Phi)$, $\Delta\Phi$ being corrective term accounting for beam bounds changes during transmission.

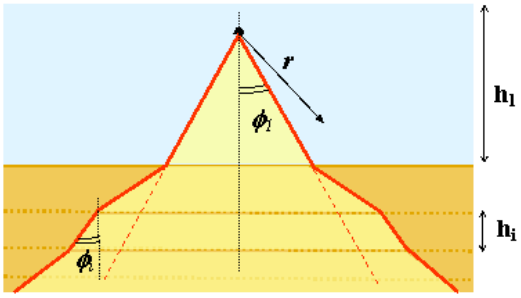

Fig.1 Ellipsoïdal wave front encountered by stratification

Reasoning with acoustic intensities, beam bounds changes are considered by comparing solid angle variation with the initial aperture:

$$n_{s,i} = \frac{(1-\cos\phi_i)}{(1-\cos\phi_1)} \qquad (1)$$

As ϕ_i is transmitted angle, $n_{s,i}$ depends on celerity variation with stratification. The corrective term is then $\Delta\Phi = \sqrt{n_{s,i}}$ (reasoning with amplitude) and the geometrical attenuation of the total backscattered field by i^e stratum is:

$$1\Big/2\left(h_1 + \sum_{k=1}^{i}\sqrt{n_{s,k}}\;h_k\right) \qquad (2)$$

In order to enable model inversion, the model needs to be fined down. Fig. 2 shows that ellipsoidal wave front can be well approximated by spherical wave propagation along stratification. Moreover, it is reminded that backscattered signals only enable to obtain layer thickness in term of two way travel time. To get the bed thickness, celerity must be known with depth. Nevertheless this parameter is unknown and, celerity in sediment is then supposed to equal water celerity to overcome this difficulty. From Fig. 2, there is less than 1,5 dB bias between the real values of celerity and their approximation in water.

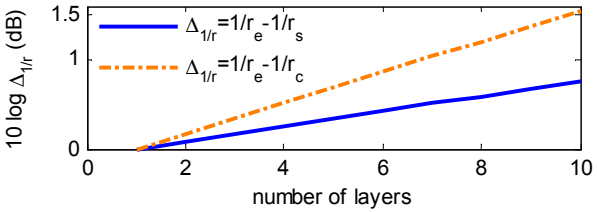

Fig. 2: Comparison of geometrical attenuation for ellipsoidal wave front $1/r_e$, spherical wave front $1/r_s$ and approximation by water celerity $1/r_c$. Initial aperture is supposed to be 30° and celerity is such as c_{i+1}=1,04 c_i.

3.2 Attenuation

Attenuation in marine sediment is modelled as follow:

$$\alpha(dB/m) = k_p\, f^n \qquad (3)$$

k_p attenuation coefficient (dB/m/khz^n), n exponent of frequency dependence, f frequency (khz)

Frequency attenuation dependence has been debated for a long time and is still under investigation as some authors support linear frequency-dependent attenuation and other authors impugn this linear frequency dependence (Table 1). To keep ability of an invertible backscattered model, it is necessary to assume linear frequency dependence. For that purpose, linear regression is applied to attenuation α (dB/m) from Eq. (3). New coefficient attenuation k_p' and b are computed in the bandwidth of chirp sonar [1 – 10] kHz and for exponent n in the interval [0,5;1,4] (Table 1).

$$\alpha'(dB/m) = k_p'\, f + b \qquad (4)$$

Relative bias between exact value α and approached value α' of attenuation has also been calculated to test validity of the linear assumption (fig. 3).

Sediment type	*k_p (dB/m/khz^n)*	*n*	*frequency (khz)*	*ref.*	*k_p' (dB/m/khz)*	*b (dB/m)*
Coarse sand	0,93	0,96	7 - 14	[6]	*0,477*	0,087
Medium sand	0,41± 0,12	1± 0,14	3,5 - 14	[6]	*0,41 ± 0,12*	0
Fine sand	0,13 0,45 ± 0,07	1,26 ± 0,13 1,04 ± 0,07	5 - 50 3,5 - 14	[7] [6]	*0,25 ± 0,08* *0,50 ± 0,09*	-0,226 -0,084
Very fine sand	0,27 0,56 0,38 ± 0,05	1,17 ± 0,13 1,00 ± 0,01 1,11 ± 0,06	5 - 50 5 - 50 3,5 - 14	[7] [7] [6]	*0,41 ± 0,13* *0,56* *0,51± 0,08*	-0,265 0 -0,219
Relatively homogenous sand	1,18 to 2,6	0,57 ± 0,05	1 - 20	[8]	*0,29 to 0,88*	1,147 to 2,526
Silt	0,3	1,05 ± 0,15	5 - 50	[7]	*0,34 ± 0,13*	-0,071
Clayey silt	0,19	0,94	7 - 14	[6]	*0,16*	0,046
Poorly sorted sediments (sand - silt -clay)	1,46	0,63 ± 0,33	0,2 - 5	[9]	*0,79 ± 0,64*	1,337
fine-grained unconsolidated sed. (sand-silt-clay, mud, turbidite)	0,055	1,12	0,01 - 500	[10]	*0,076*	-0,035

Table 1: Attenuation of saturated sediment from the literature. Values in grey computed by the writer of this report

In the bandwidth of subbottom profilers, hypothesis of linear frequency-dependent attenuation might be acceptable for any exponent n included in [0,4;1,25]. At frequencies lower than 2,3 khz, linear approximation induces error greater than 10% for values of exponent n near 0,4 and 1,4. As most of exponent values are concentrated within interval [0,4;1,25], linear approximation of attenuation frequency dependence is acceptable and used in the coherent backscattering model.

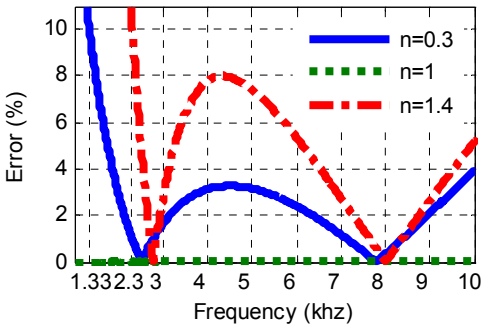

Fig.3 Percent error between "exact attenuation model" and "linear attenuation model" 100 (α'-α)/α

3.3 Rugosity

Examined rugosities are supposed to be normally distributed. This hypothesis offers a good compromise between experiment fitting [11] and modelling complexity. This roughness may refer to surfaces shaped by erosion or grain sizes (excluding ripples). Under the assumption of a gaussian rugosity spectrum, roughness standard deviation is the one rugosity parameter and Eckart's model [12] can be used to analyse impact of microroughness (P<<1) on coherent reflected field (resp. transmitted field) using Rayleigh parameter P in Eq. (5) (resp. rugosity parameter P_T in Eq. (6) in transmission [13]):

$$V_{rough} = V_{smooth}\, e^{-\frac{P^2}{2}}, \qquad P = 2k_i \sigma \cos\theta_i \quad (5)$$

$$T_{rough} = T_{smooth}\, e^{-\frac{P_T^2}{2}}, P_T = k_{i+1}\sigma\left(\frac{c_{i+1}}{c_i}\cos\theta_i - \cos\theta_{i+1}\right) \quad (6)$$

σ rugosity standard deviation, k_i wave number, θ_i incidence angle, c_i celerity in medium i

This small rugosity modelling has been validated by laboratory experiments (LMA, Marseille) which have also enabled to analyse the little-know case of fair rugosity (P≈1 and λ>>σ) and to deduce that coherent reflection still prevails although incoherent returns induced by surface's scatterers are visible on echo's tail. Measures have been conducted on a plate with a gaussian rugosity spectrum (standard deviation σ = 0,06 mm). To restore conditions of intermediate rugosity P≈1 and λ>>σ, reflected and transmitted fields were measured at 2,25 MHz.

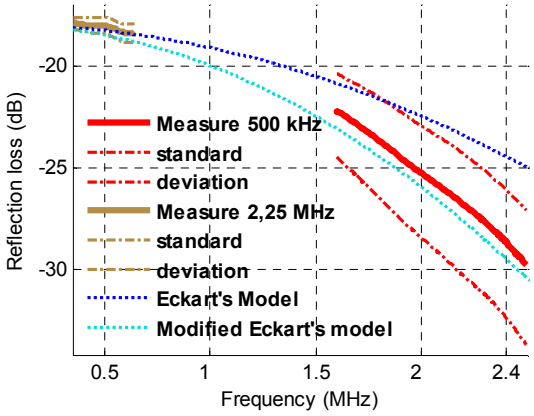

Fig. 4 Impact of fair rugosities on reflection loss

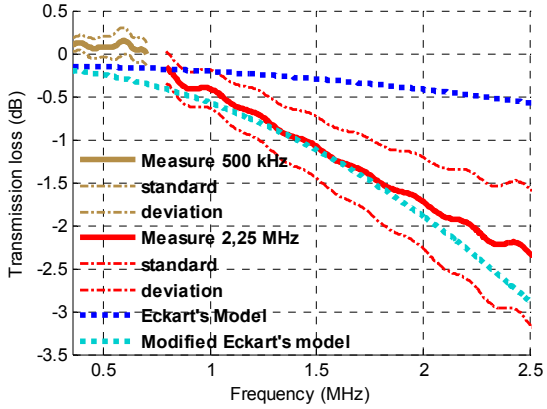

Fig. 5: Impact of fair rugosities on transmission loss

From these measurements, a similar model than the one of Eckart has been empirically established to simulate wave's reflection (Fig. 4, Eq. (7)) and transmission (Fig. 5, Eq. (8)) through fairly rough surfaces while introducing corrective terms on rugosity parameters:

$$P = \frac{4}{3} 2k_i \sigma \cos\theta_i \quad (7)$$

$$P_T = \frac{5}{2} k_{i+1} \sigma \left(\frac{c_{i+1}}{c_i}\cos\theta_i - \cos\theta_{i+1}\right) \quad (8)$$

P modified rugosity parameter in reflection, P_T modified rugosity parameter in transmission.

These formulas will be inserted in the global backscattering model.

3.4 Volumetric heterogeneity: continuous impedance variation

As stated in section 2.2, physical properties may vary gradually inside bed sediment. This phenomen has been observed at the water/seafloor interface with the presence of a transitional layer with thickness from 0,5 cm to 10 cm. Continuous variation of sediment parameters may also happen for buried bed (thickness from 1cm to 20cm). Within first hundred meters, celerity fluctuates between 1500m/s and 1800m/s [14] whereas density varies more from 1300kg/m^3 to 2000kg/m^3 for smooth sediments. Impact of changing parameters on acoustic signal propagation is then examined while using transfert function method [15] to model continuous impedance variation. Under our assumptions of spherical wave propgation and instrumentation sensitivity to specular reflection and transmission, this method is well adapted to our problem as it is easy to implement and potentially invertible.

Defining an inhomogeneous medium between two homogeneous layers, transfert function links acoustic fields at each extremity of the inhomogeneous layer Eq. (9):

$$\begin{bmatrix} p^+(x_a) \\ p^-(x_a) \end{bmatrix} = \begin{bmatrix} m_{11} & m_{12} \\ m_{21} & m_{22} \end{bmatrix} \begin{bmatrix} p^+(x_b) \\ p^-(x_b) \end{bmatrix} \quad (9)$$

Supposing that impedance follows an exponential variation due to exponential evolution of density (celerity and attenuation remain constant within inhomogeneous layer), reflection (Eq. (10)), transmission (Eq. (11)) coefficients are derived from this transfer function:

$$R = p^-(x_a)/p^+(x_a) = m_{21}/m_{11} \quad (10)$$

$$T = p^+(x_b)/p^+(x_a) = 1/m_{11} \quad (11)$$

with

$$m_{11} = e^{-\beta_0 \Delta x}\left[\cos[k^*(\omega)\Delta x] + \frac{ik(\omega)}{k^*(\omega)}\sin[k^*(\omega)\Delta x]\right]$$

$$m_{21} = e^{-\beta_0 \Delta x}\frac{\beta_0}{k^*(\omega)}\sin[k^*(\omega)\Delta x] \quad (13)$$

And $\beta_0 = c\ln(\rho_2/\rho_1)/2\Delta x$

$$k^*(\omega) = \left[k^2(\omega) - \beta_0^{\,2}\right]^{1/2} \quad (14)$$

$$k(\omega) = \omega/c(\omega) - i\alpha(\omega)$$

Transmission loss and reflection loss are calculated for a media with exponential density variation from 1000kg/m^3 to 1500kg/m^3, constant celerity c=1500 m/s and constant attenuation coefficient k_p=0,3 dB/m/kHz (Fig. 6).

For small thickness (Δx = 0,01 m), transitional layer is invisible and bottom loss refers to reflection loss between the two homogeneous media bordering transitional layer (Fig. 6). This case happens when $\lambda/\Delta x \geq 4{,}5$ defined for a maximal reflection loss fall of 3dB.

When the inhomogeneous bed is large (Δx =0,1 m), reflected energy is very low and most of acoustic energy is transmitted and absorbed in the medium. Up to a reflection loss drop of 10 dB, reflection coefficient can be approached to zero and this case happens when $\lambda/\Delta x \leq 2{,}6$.

For intermediate thickness bed (Δx =0,05 m), backscattering is strongly affected by gradual changes of impedance: reflection loss declines of 10 dB within the frequency bandwidth [1–10] khz. Thus, impact of transitional layer is inserted in the coherent backscattering model, and a special attention is given on analysis of intermediate thickness bed defined for $2{,}6 \leq \lambda/\Delta x \leq 4{,}5$ (from 4 cm to 7 cm at 10 khz).

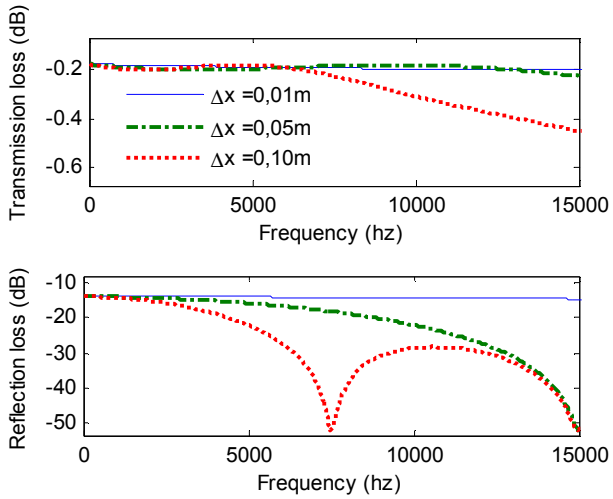

Fig.6 Reflection loss $R_L=|R|^2$ and transmission loss $T_L= Z_1/Z_2\ |T|^2$ calculated for several thicknesses Δx of transitional layer

All the examined bottom parameters are now introduced in the global backscattering model which is presented in the next section.

4 Coherent backscattering model

Seafloor is viewed by chirp sonar as a layered attenuated medium with rough interfaces and eventual continuous varying parameters. Coherent backscattering impulse response of seafloor is then modelled while using multilayered model [2] and inserting bottom parameters studied above Eq. (15):

$$p_r(\omega) = \frac{p_0}{2c_1}\left\{\sum_{i=1}^{n}\left[\frac{e^{-j\omega f \tau_i}}{\tau_i}V_i\prod_{k=1}^{i}H_k{}^2 T_{k-1,k}T_{k,k-1}\right]\right\} \quad (15)$$

with H_i transfert function of the i^e homogeneous layer (Eq. 16), V_i reflection coefficient (Eq. (17)), $T_{i-1,i}$ $T_{i,i-1}$ transmission coefficients (Eq. (18) and Fig. 7).

$$H_i(\omega) = e^{-ln(10)/20\, k_{p,i} f\, c_i \tau_i} \quad (16)$$

$$V_i(\omega) = r_{1,i+1} + t_{1,i+1}t'_{1,i+1}r_{t,i+1} + t_{1,i+1}t'_{1,i+1}t_{2,i+1}t'_{2,i+1}r_{2,i+1} \quad (17)$$

If i =1: $T_{i-1,i}T_{i,i-1} = 1$ and for i > 1:

$$T_{i-1,i}(\omega) = t_{1,i}t_{2,i}t_{t,i} \text{ and } T_{i,i-1}(\omega) = t'_{1,i}t'_{2,i}t'_{t,i} \quad (18)$$

Coefficients $r_{1,i+1}$, $r_{2,i+1}$ and $t_{1,i}$, $t_{2,i}$, $t'_{1,i}$, $t'_{2,i}$ are calculated via Snell-Descartes laws and via Eq. (5) and (6) or Eq. (7) and (8) for rough surfaces. r_t (resp. t_t) is reflection (resp. transmission) coefficient of transitional layer (Fig. 7) and is calculated via Eq. (10) (resp. Eq. (11)).

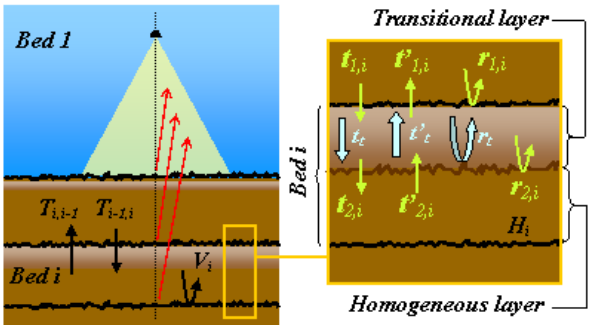

Fig.7 Parameterisation of seafloor

Then, for a specific emission, backscattered field is:

$$y(\omega) = p_r(\omega)\cdot x(\omega) \quad (19)$$

Backscattering field has been calculated for two subbottom configurations (Table 2) and for two emission chirp of time duration t_p=0,01s and with frequency bandwidth: [1,7 – 5,2] kHz centred at 3,5 kHz and [5-15] kHz centred at 10 kHz (Fig. 8 and Fig. 9).

	1	Parameters	2	Parameters
Bed 1 *water* 20m		ρ_1 = 1 g/cm^3 c_1 = 1500 m/s	σ_1 = 1 cm	ρ_1 = 1 g/cm^3 c_1 = 1500 m/s
Bed 2 2 m		ρ_2 = 1,3 g/cm^3 c_2 = 1600 m/s	0,05m	$\rho_{t,2}$ = 1 to 1,3 g/cm^3 $c_{t,2}$ = 1600 m/s ρ_2 = 1,3 g/cm^3 c_2 = 1600 m/s
Bed 3 1,5 m		ρ_3 = 1,8 g/cm^3 c_3 = 1725 m/s $k_{p,3}$ = 0,1 dB/m/kHz	σ_3 = 2 cm	ρ_3 = 1,8 g/cm^3 c_3 = 1725 m/s $k_{p,3}$ = 0,1 dB/m/kHz
Bed 4 2 m		ρ_4 = 2 g/cm^3 c_4 = 2200 m/s		ρ_4 = 2 g/cm^3 c_4 = 2200 m/s

Table 2: Tested seafloor layout

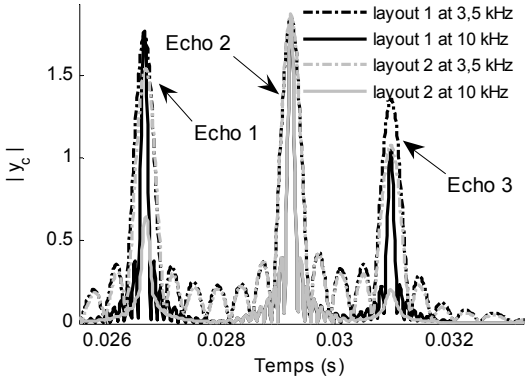

Fig. 8 Compressed backscattered field $y_c = TF^{-1}\left(y(\omega)\cdot\overline{x(\omega)}\right)$

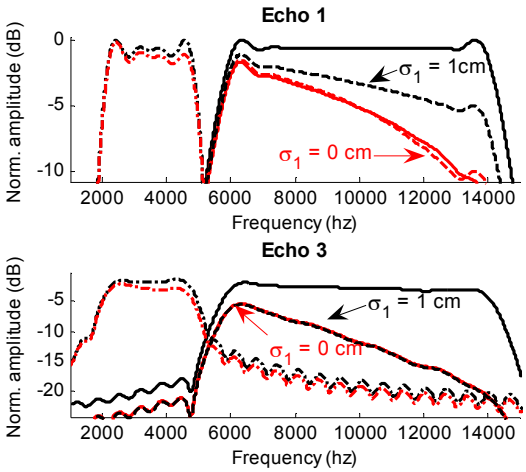

Fig. 9 Frequency spectrums of echo 1 and echo 3, black line: layout 1 and red line: layout 2. The three spectrums of echo 3 with σ=1cm and σ=0cm are superimposed.

As expected, signal is less sensitive to absorption (Fig. 8, Echo 3 & layout 1), rugosity and layer with varying parameters (Fig. 9) at low frequency. Rough interfaces and transitional layer do not affect signal transmission (Fig. 8, Echo 2 & layout 2) whereas reflection is disturbed by of fair rugosities and transitional bed of intermediate thickness. If parameters continuously vary in a large distance, any signal is reflected. Moreover, Fig. 9 (Echo 1) shows that impact of transitional layer with intermediate thickness prevails rugosity's influence.

5 Discussion and conclusion

The presented backscattering model takes into account bottom layering, attenuation, interfering and transitional layer with small and fair rugosity. To summerize, reflection is sensitive to intermediate thickness layer with continuous varying parameters and to fair rugosity whereas attenuation does not significantly modify it. Regarding with transmission, slightly and fairly rough interfaces are well approached by smooth surfaces and transmission is total through transitional layer of large and intermediate thickness. Attenuation is the predominating transmission parameter. Thus, for inversion, assumption of a layered homogeneous attenuated media is valid for transmission into overlying layer for any rough interfaces (small or fair rugosity) and any thickness of transitional layer. Reflection loss and standard deviation rugosity may be calculable for fair rough reflecting interface. If rugosity is conjugated with intermediate thickness of transitional layer, rugosity is not assessable and reflection loss is sorely calculable.

Acknowledgments

The authors would like to thank the LMA from Marseille and Prof. Jean-Pierre Sessarégo for his cooperation.

References

[1] E. L. Hamilton, ''Geoacoustic Modelling of the sea floor", *J. Acoust. Soc. Am. 68*,1313- 1340 (1980)

[2] L. M. Brekhovskik, Yu. P. Lysanov, "Fundamentals of Ocean Acoustics", Springer, 3° ed. (2003)

[3] B. Langli, J-C. Le Gac, "The first results with a new multibeam subbottom profiler", *Proceedings Ocean'04 MTS/IEEE* 2, 1147-1153 (2004)

[4] S. Rakotonarivo, M. Legris, R. Desmare, F. Jean, "Impact of measurement geometry on quantitative characterisation of sediment with high-resolution sub-bottom profiling systems (1 kHz – 15 kHz)", *Proceedings SeaTechWeek '06* (2006)

[5] Gary Nichols, "Sedimentology and stratigraphy", Blackwell Science (1999)

[6] E. L. Hamilton, ''Compressional-Wave attenuation in Marine sediments'', Geophysics 37, 620-646 (1972)

[7] C. Mc Cann, D. M. Mc Cann, "The attenuation of compressional waves in marine sediments", Geophysics 34, 882 – 892 (1969)

[8] M. A. Zimmer, L. D. Bibee, M. D. Richardson, "Frequency dependent sound speed and attenuation measurents ins seafloor sands from 1 to 400 kHz", *Proceedings Boundary Influences in High Frequency, Shallow Water Acoustics*, 57 -64 (2005)

[9] E. I. Best, Q. J. Huggett, A. J. K. Harris, "Comparison of in situ and laboratory acoustic measurements on Lough Hyne marine sediments", *J. Acoust. Soc. Am. 110*, 695-709 (2001)

[10] F. A. Bowles, "Observations on attenuation and shear-wave velocity in fine-grained, marine sediments", J. Acoust. Soc. Am. 101, 3385-3397 (1997)

[11] S. Leconte, X. Lurton, B. Marsset, D. Gibert, ''Seabed roughness evaluation using subbottom profiler signal analysis", *Proceedings SeaTechWeek '04* (2004)

[12] C. Eckart, "The scattering of sound from the sea surface", J. Acoust. Soc. Am. 25, 566-570 (1953)

[13] P. B. Nagy, L. Adler, "Surface roughness induced attenuation of reflected and transmitted ultrasonic waves", *J. Acoust. Soc. Am. 82*, 193- 197 (1987)

[14] E. L. Hamilton, ''Sound velocity gradients in marine sediments", *J. Acoust. Soc. Am. 65*, 909- 922 (1978)

[15] J. Bai, C. Rorres, P. D. Pedersen, O. L. Tretiak, "Direct acoustic scattering for one dimensional lossy media", *J. Acoust. Soc. Am. 78*,1375- 1383 (1985)